Supplementary Information for

Disruption of Proteostasis Causes IRE1 Mediated Reprogramming of Alveolar Epithelial Cells

Jeremy Katzen, Luis Rodriguez, Yaniv Tomer, Apoorva Babu, Ming Zhao, Aditi Murthy, Paige Carson, Matthew Barrett, Maria C Basil, Justine Carl, John P Leach, Michael Morley, Matthew D McGraw, Surafel Mulugeta, Timothy Pelura, Glenn Rosen, Edward E Morrisey, Michael F Beers

Michael F Beers
Email: mfbeers@pennmedicine.upenn.edu

This PDF file includes:

Supplementary Materials and Methods
Figures S1-S12
Table S1-2

SUPPLEMENTARY MATERIALS AND METHODS

Bleomycin lung injury and pharmacological interventions in mice

Mice were anesthetized with isoflurane and intubated followed by intratracheally instillation of bleomycin (3 U/Kg) in normal saline at a concentration of 1U/mL. Equal volume normal saline was instilled intratracheally as controls. Bortezomib (Calbiochem CAS 179324-69-7) was dissolved in DMSO (100mg/mL), suspended in normal saline (at 0.1% DMSO) and dosed by IP injection once at 1mg/kg (vehicle = 0.1% DMSO in normal saline), a dose selected for lack of toxicity in control animals in a single dose. For experiments in the *Sftpc*^{C185G} model, BTZ was given 48 hours following OG TMX mutation induction. For bleomycin experiments, BTZ was given concurrently with intratracheal bleomycin.

The dual IRE1α kinase and RNase inhibitor OPK-711 was provided by OptiKira and resuspended in vehicle (30% propylene glycol, 5% Tween 80, 65% D5 water, pH 4.0 at 20mg/mL) and dosed by OG daily at 20mg/kg, a dose selected based on successful inhibition of *Xbp1* splicing in *Sftpc*^{C121G} AEC2s.

BALF analysis

BALF cells from the 5mL lavage were pelleted, resuspended in 1mL of normal saline and quantified by Z1 Coulter Counter (Beckman Coulter). BALF cell differential cell counts were obtained by manually quantifying >200 cells in 5 20x fields of cytospins of BALF cell pellets stained with modified Giemsa (Sigma Aldrich, #GS500). Aliquots of first mL, cell free BALF were analyzed for protein content by the Lowery method, and cytokines were measured using CXCL1, CCL11, CCL17 ELISA kits (R&D Systems).

Large-aggregate surfactant fractions were prepared by ultracentrifugation of the 5mL lavage volume as previously described (1), and resuspended in 40uL of normal saline. Equal volumes (5uL) of the resuspended large-aggregate surfactant pellet per mouse was subjected to western blot analysis as described in detail below.

Lung Histology and Immunofluorescence Staining

Lungs were fixed by tracheal instillation of a 1.5% glutaraldehyde/1.5% paraformaldehyde mixture in 0.15 M HEPES buffer at a constant pressure of 25 cm H2O and removed en bloc. Fixed lungs were embedded in paraffin, and for histopathology, 4 µm thick sections were prepared and stained with hematoxylin and eosin. Imaging was performed on a Nikon Eclipse 80i at 4x and 10x magnification and processed and analyzed on ImageJ.

Unstained sections were stained with the following primary antibodies: In-house rabbit anti-proSP-C (NPRO2 1:200), In-house rabbit anti-SPB (PT3 1:200), Rat anti-Krt8 (DHBS Troma-I AB_531826, 1:200), Rabbit anti-Claudin 4 (Thermo Fischer Scientific 36-4800, 1:200), Rat anti-Lamp3 (Novus Bio DDX0191P-100 1:200). Secondary antibodies were obtained from Jackson Immunochemicals: Goat anti-mouse 594 (115-585-146), Goat anti-rabbit 594 (111-585-144), Goat anti-mouse 488 (115-545-062), Goat anti-rabbit 488 (111-545-144), Goat anti-rat 594 (112-585-003). DAPI (Invitrogen, D3571) was used for nuclear staining, and sections were mounted with Mowiol (Sigma-Aldrich, 81381).

ProSP-C+ and Krt8+ cells were quantified by manually counting cells in 4 20x fields per biological replicate. AEC2 ProSP-C mean fluorescence intensity (MFI) in BTZ and vehicle treated mice at 4 and 7 days was assessed by measuring individual cell MFI for all ProSP-C+ cells in 3 20x fields per mouse. The MFI of the 40 most fluorescent cells per 20x field (120 cells per mouse in the 3 fields) are presented as proSP-C MFI per AEC2 in Figure 2H.

Multichannel flow cytometry of mouse lung

Tissue neutrophil quantification was performed by *flow cytometry.* as previously described (2). Lungs were digested in DMEM + 5% FBS + 2 mg/ml Collagenase D (catalog 11088866001, Roche), passed through 70-µm nylon mesh to obtain single-cell suspensions, and then mixed with RBC Lysis Buffer

(A10492-01, Thermo Fisher Scientific). Cell pellets were resuspended in PBS + 0.1% sodium azide and blocked with anti–mouse CD16/32 antibody (Fc block, eBiosciences), followed by incubation with antibody mixtures with CD45 (Biolegend 103130), SiglecF (BD Biosciences 562757), Ly6G (Biolegend 127622), CD11b (Biolgend 101235) (or isotype controls) and conjugated viability dye (eBioscience 65-0865-14). Single-cell suspensions were then analyzed on an LSR Fortessa (BD Biosciences). They were then gated on viability and singlets and analyzed with FlowJo software (FlowJo LLC). Neutrophils were identified as CD45+/Live, SiglecF^{low}, Ly6G^{hi}, CD11b^{hi}.

AEC2 western blotting and proteasome activity assay

AEC2 protein lysate was collected and subjected to western blot. SDS-PAGE using Novex Bis-Tris gels (NP0301, Thermo Fisher Scientific) and immunoblotting of PVDF membranes with primary antisera (see *SI Appendix*, Table S1 for antibody list) followed by species-specific horseradish peroxidase–conjugated secondary antisera were performed as previously published (1)**.** Bands detected by enhanced chemiluminescence (ECL2 80196 Thermo Fisher Scientific or WesternSure 926-95000, LI-COR) were acquired by direct scanning using an LI-COR Odyssey Fc Imaging Station and quantitated using the manufacturers' software.

AEC2 proteasome activity (chymotrypsin-like activity) was measured using the Proteasome-Glo Assay System (Promega, G8621) as per kit instructions. Briefly, AEC2 cell lysate was prepared as above, protein content was measured using Lowery assay. 50uL of AEC2 lysate was combined with Proteasome-Glo Reagent (luciferin detection reagent and the Chymotrypsin-Like proteasome substrate) and incubated for 30 minutes, followed by luciferin detection using a Promega Glomax Multi+ Detection Unit E8032. Luminescence (RFU) was divided by AEC2 lysate protein content (ug) for a relative chymotrypsin-like activity (RFU/ug).

AEC2 RT-qPCR and RNA sequencing

For RT-qPCR, mouse AEC2s were sorted and RNA was extracted using RNeasy Mini kit (Qiagen, Cat #74174), and converted to cDNA using the Verso CDNA Synthesis Kit (Thermo, AB1453B). RT-qPCR was performed on a QuantStudio 7 Flex Real-Time PCR System Library with primers listed in *SI Appendix*, Table S2. Differential expression was calculated as a fold-increase using ΔΔCt method with normalization to *18s*.

For RNA sequencing, mouse AEC2s were sorted and RNA extracted as above. Library prep was performed by GeneWiz, LLC. Fastq files were evaluated for quality control with the FastQC program and then aligned against the mouse reference genome (mm9) using the STAR aligner (3)**.** Duplicate reads were flagged with the MarkDuplicates program from Picard tools and excluded from analysis. Per gene read counts for Ensembl (v67) gene annotations were computed using the R package Rsubread. Gene counts, represented as counts per million (CPM), were nominalized using TMM method in the edgeR R package, and genes with 25% of samples with a CPM < 1 were considered low expressed and removed. The data were transformed with the VOOM function from the limma R package to generate a linear model and perform differential gene expression analysis (3). We employed the empirical Bayes procedure as implemented in limma to adjust the linear fit and to calculate *P* values given the small sample size of the experiment. We adjusted *P* values for multiple comparisons using the Benjamini-Hochberg procedure. PCA, volcano plots, and heatmaps were generated in R package. Kyoto encyclopedia of genes and genomes (KEGG) pathway enrichment analysis was performed using the online based software ToppGene (https://toppgene.cchmc.org/enrichment.jsp) based on differentially enriched genes (FC >1.5 P-value <0.05) (4).

EPCAM enriched single cell RNA sequencing and analysis

To enrich for EPCAM+ cells from the *Sftpc*^{C121G} model, a single cell suspension was prepared from two (one male and one female) *Sftpc*^{C121G} mouse at Day 0 (*Sftpc*^{C121Gneo}), Day 3, and Day 7 by physical and enzymatic dissociation followed by MACS sorting by LS columns (Miltenyi Biotec 130-042-401) with CD45+ cell removal using CD45 micobeads (Miltenyi Biotec 130-052-301) followed by EPCAM+ cell enrichment using EPCAM microbeads (Miltenyi Biotec 130-105-958). The male and female biological replicates for each timepoint were combined in equal proportions into a single suspension and the EPCAM+ enriched combined cell suspension were loaded onto individual GemCode instrument (10X Genomics), one for each of the three timepoints. Single-cell barcoded droplets were produced using 10X Single Cell 3' v3 chemistry. The libraries that were generated were sequenced on an Illumina HiSeq2500 instrument in a High Output mode. Single cell RNA-Seq reads were aligned to mouse genome (mm10/GRCm38) using STARSolo (version 2.7.5b) (5). For further processing, integration and downstream analysis, SeuratV3 was used (6). Cells that express less than 200 genes and/or genes greater than 3 Median absolute deviation above the median were filtered out. Cells that had greater than 10% mitochondrial counts were also removed. The cell cycle phase score was calculated using CellCycleScoring function in Seurat and data was normalized and scaled using the SCTransform function, adjusting for cell cycle, percent mitochondria, and number of UMI per cell. Integration of the individual samples were performed using the normalized counts from SCTransform and the top 3000 variable genes as anchors. Linear dimension reduction was done using PCA, and the number of PCA dimensions was evaluated and selected based on the assessment of the ElbowPlot. Data was clustered using the Louvain graph-based algorithm in Seurat at an appropriate cluster resolution. The Uniform Manifold Approximation and Projection (UMAP) dimension reduction algorithm was used to project the cells onto two-dimensional space for visualization. The cell populations were identified using either known canonical marker genes or by the assessment of the cluster-defining genes based on differential

expression using the FindMarkers function in SeuratV3. Alveolar clusters were subsetted and clustering and UMAP reduction was reperformed (Fig. 5). For intra-cluster gene expression differences, the FindAllMarkers function was used to identify variation between specified clusters. Heatmaps were generated per cluster or with cells arranged in pseudotemporal ordering across the X axis, and were made using the ComplexHeatmap R package (7). Trajectory analysis was performed on the UMAP reduction using the R slingshot package with homeostatic AEC2 cluster as the starting point and without assigned endpoints (8).

Gene ontogeny analysis for enriched biological processes was performed using the online based software ToppGene (https://toppgene.cchmc.org/enrichment.jsp) based on differentially enriched genes between the UPR activated cluster and the two other AEC2 clusters (homeostatic and reprogrammed state) and between reprogrammed state cluster and the two other AEC2 clusters (homeostatic and UPR activated cluster) (4). Enriched genes were defined as those with $Log_2FC > 0.25$ and adjusted P-value <0.05.

MLE12 Culture

For characterization of the processing of SP-C BRICHOS domain cysteine mutations MLE12 cells were grown to 75% confluence and incubated overnight in optimem media (Invitrogen) with indicated plasmid DNA/Lipofectamine complexes as previously described (9). At 24 hours following transfection MLE12 cell lysate were collected for western blot analysis. As a positive control for UPR activation in mouse AEC2 western blots, MLE12 cells were treated for 16 hours with 1mg/mL Tunicamycin (Sigma, T7765).

To assess for the consequence of activating IRE1/XBP1s signaling in MLE12 cells we used IXAV4 at 10uM, which has been shown to selectively activate IRE1α signaling without stimulating the other UPR branches, and specifically the IRE1α RNase activity without activating IRE1α RIDD or kinase activity (34). MLE12 cells were grown to 100% confluence and treated overnight with IXAV4 and harvested at 24 hours for RNA analysis by RT-qPCR as described above. To assess for optimal OPK-711 concentration for the primary mouse AEC2 organoid experiments, MLE12 cells were grown to 75% confluence and incubated overnight in optimem media (Invitrogen) with indicated plasmid DNA/Lipofectamine complexes concurrently with the indicated concentrations of OPK-711. At 24 hours following transfection MLE12 were harvested for RNA analysis of *sXbp1* expression by RT-qPCR as described above.

Primary mouse AEC2 Organoid Culture

Inducible *Sftpc*^{C121Gneo} AEC2 were isolated from mouse lungs and quantified using Z1 Coulter Counter. In each technical replicate, 5×10^3 AEC2 were combined with 5×10^4 primary mouse lung fibroblasts in 50% Matrigel (Corning, catalog # 356231) and 50% MTEC-SAGM (Lonza, catalog # CC-3118, prepared as previously described (10)) in a Falcon Cell Culture Insert (Thermo Fisher Scientific, catalog # 08770). Cell/matrigel suspension solidified and MTEC-SAGM media was then added into the bottom of the well. Media was changed every other day. 10 μM rock inhibitor (Y-27632 dihydrochloride, Millpore Sigma, catalog # Y0503) was added to the media for the first two days of culture. At Day 10, media was changed in select wells to include 4OH-Tamoxifen (Sigma, H6278) suspended at 1uM in 100% EtOH a final concentration of 500nM (0.05% EtOH), 4OH-Tamoxifen with OPK-711 suspended in DMSO (10mM) for final concentration of 200nm (0.1% DMSO), 4OH-Tamoxifen with ISRIB (Sigma, SML0843) in DMSO (2mM) for a final concentration of 200nm (0.1% DMSO), or the combined vehicles (0.05% EtOH +0.1%

DMSO). On the final day of culture (day 14), organoids were removed from transwell inserts by dissociating the matrigel with dispase. RNA was isolated and analyzed by RT-qPCR.

SUPPLEMENTAL FIGURES

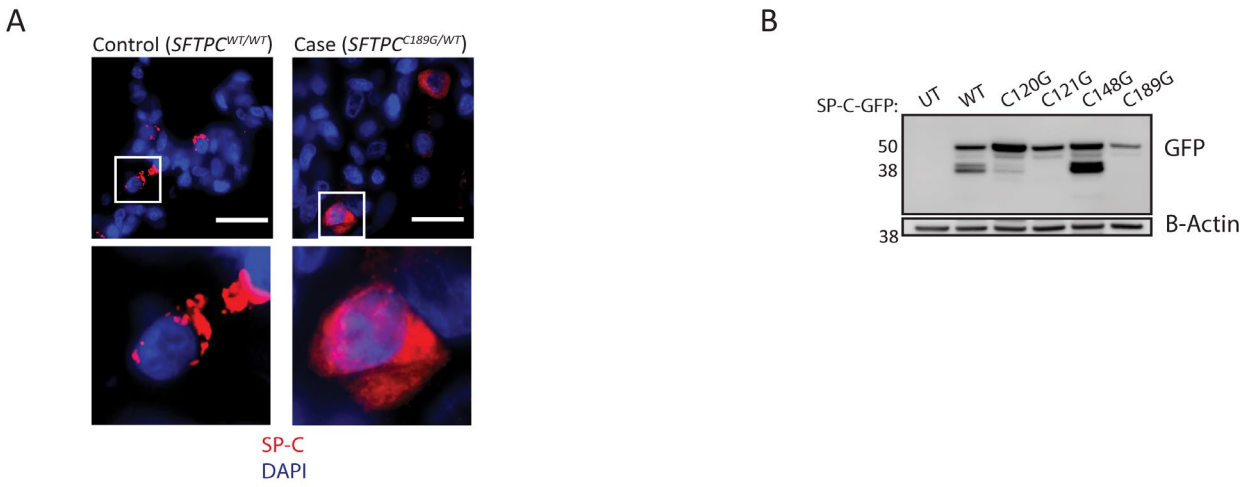

Figure S1. **Modeling a clinical *SFTPC* BRICHOS mutation**
(**A**) Immunostaining of lung sections from a patient carrying the *SFTPC*^{C189G} mutation and aged matched (4 week) control for proSP-C shows cytosolic punctae in control section and a reticular pattern in the case (60x magnification scale bar = 20uM). (**B**) Western blotting for GFP in MLE12 cell lysates 24 hours after transfection with *SFTPC* plasmids, showing absence of a lower molecular weight band in the C121G and C189G transfections indicating proximal retention and incomplete processing of proSP-C with these mutations (UT=untransfected).

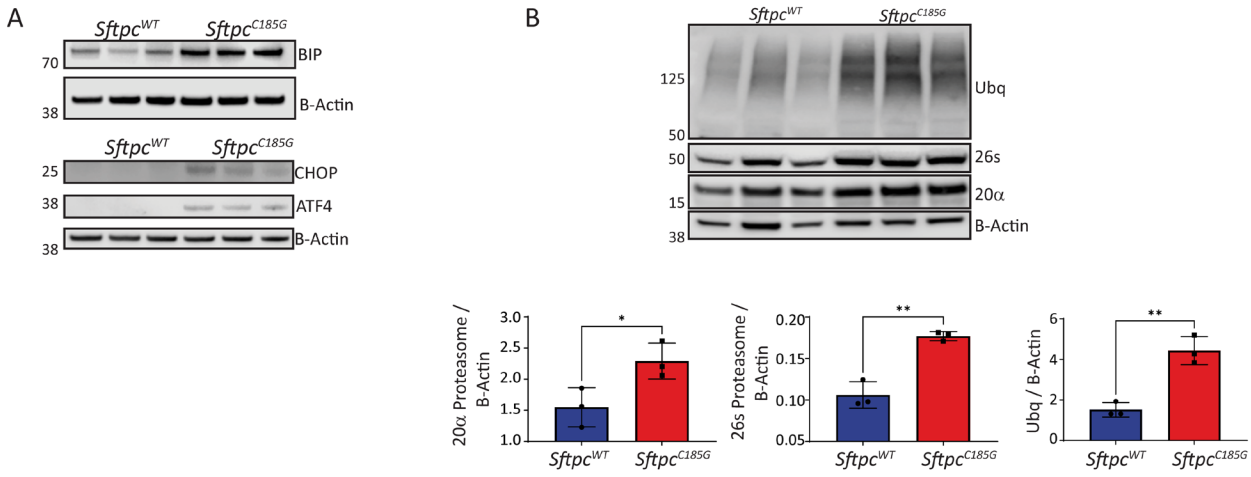

Figure S2. **In Vivo expression of a clinical Sftpc mutation challenges AEC2 proteostasis and activates the UPR despite increases in proteasome mass**

(**A**) Western blotting analysis for BIP (top) and ATF4 and CHOP (bottom) in *Sftpc*^{WT} and *Sftpc*^{C185G} lysates of AEC2 isolated 7 days post-TMX. (**B**) (**top**) Western blotting and (**bottom**) densitometry for Polyubiquitin (Ubq) and the 20α and 26s proteasome subunits in *Sftpc*^{WT} and *Sftpc*^{C185G} AEC2 cell lysates 7 days post-TMX.

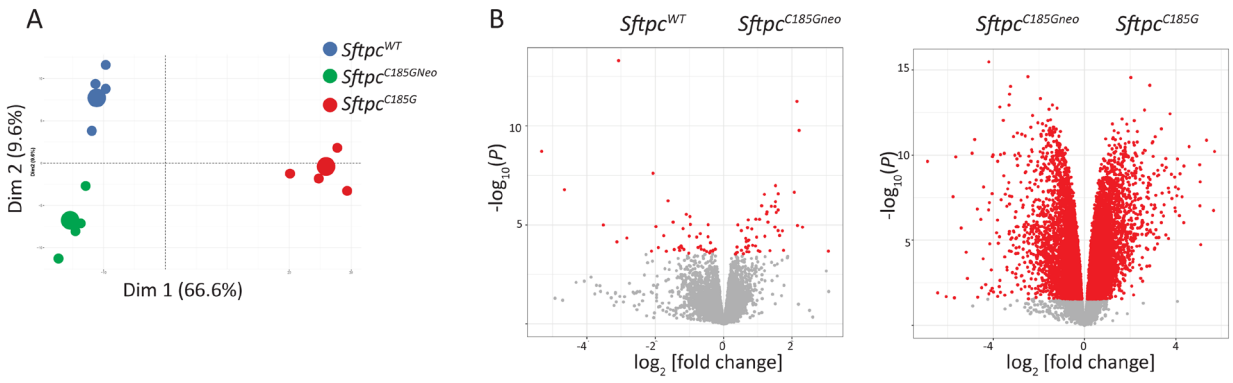

Figure S3. RNA sequencing of AEC2s isolated from *Sftpc* mutation model

(**A**) PCA plot of AEC2 bulk RNA sequencing shows separation of the *Sftpc*^{C185G} samples from both the *Sftpc*^{C185Gneo} founder line and the *Sftpc*^{WT} samples. (**B**) Volcano plots showing differentially expressed genes in AEC2 between the indicated *Sftpc* genotypes. (red= >1.5 fold change, Adj P value < 0.05).

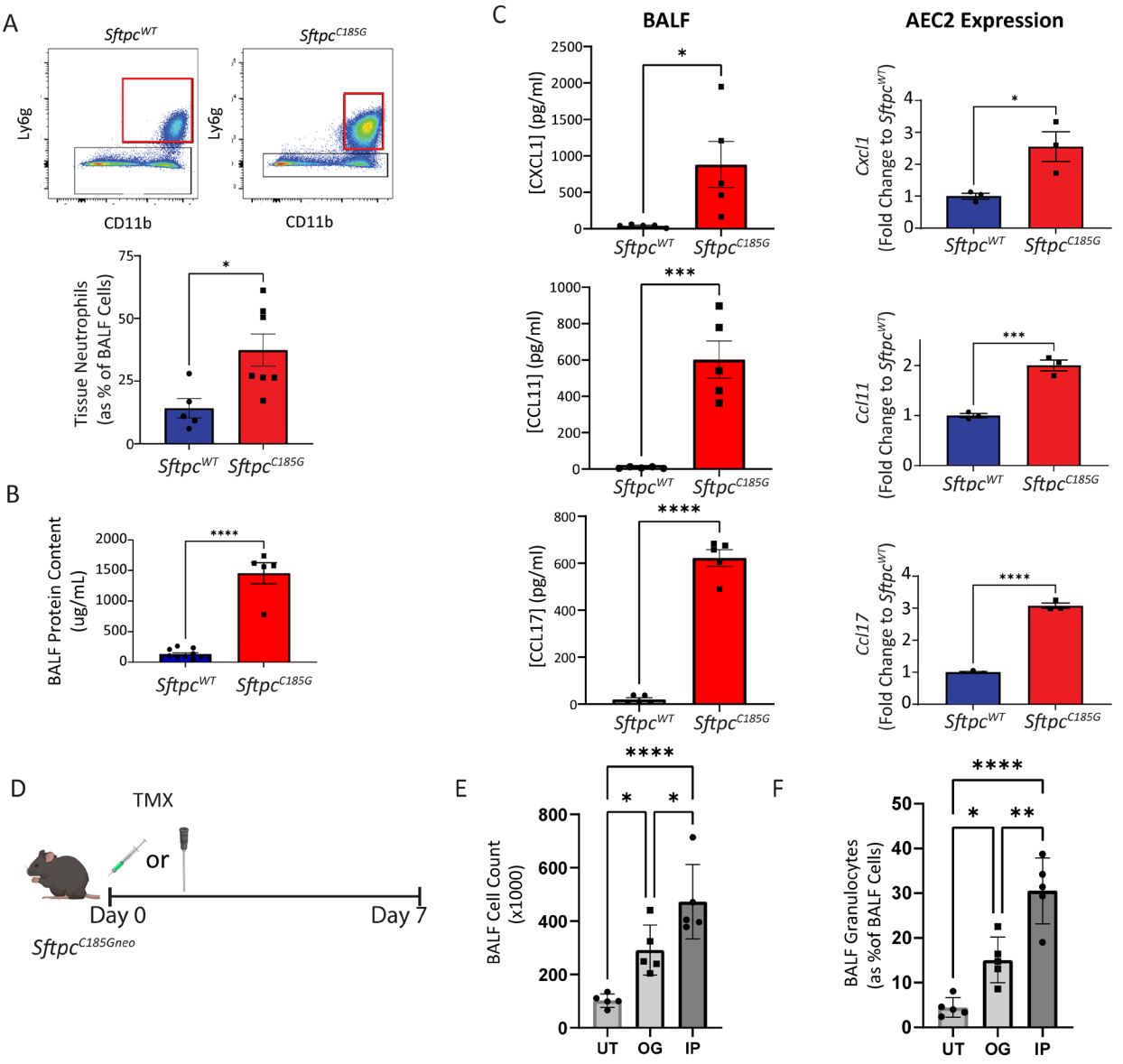

Figure S4. ***Sftpc* mutant AEC2s drive recruitment of granulocytes**

(**A**) (**top**) Representative flow cytometry gating used to identify Ly6g high Cd11b high neutrophils. (**bottom**) Quantification of tissue neutrophils expressed as a percentage of total lung CD45+ cells in *Sftpc*^{WT} and *Sftpc*^{C185G} lungs 7 days post-TMX. (**B**) BALF protein as measured by the Lowry assay in *Sftpc*^{WT} and *Sftpc*^{C185G} mice. (**C**) (**left column**) BALF cytokines CXCL1, CCL11, CCL17 quantified by ELISA in *Sftpc*^{WT} and *Sftpc*^{C185G} BALF samples from 7 days post-TMX. (**right column**) q-RT-PCR for *Cxlc1*, *Ccl11*, *Ccl17* from *Sftpc*^{WT} and *Sftpc*^{C185G} AEC2 isolated 7 days post-TMX. (**D**) Schematic for comparison of intraperitoneal (IP) and oral gavage (OG) delivery of TMX. (**E**) BALF cell counts and (**F**) percentage of BALF cells that are granulocytes by manually counting Giemsa stained cytospins from *Sftpc*^{C185G} not receiving TMX (untreated—UT) and *Sftpc*^{C185G} mice at 7 days after IP or OG TMX shows attenuated alveolitis with OG TMX delivery compared to IP. *p < 0.05, ***p < 0.0005, ****p < 0.0001 by two-way t-test.

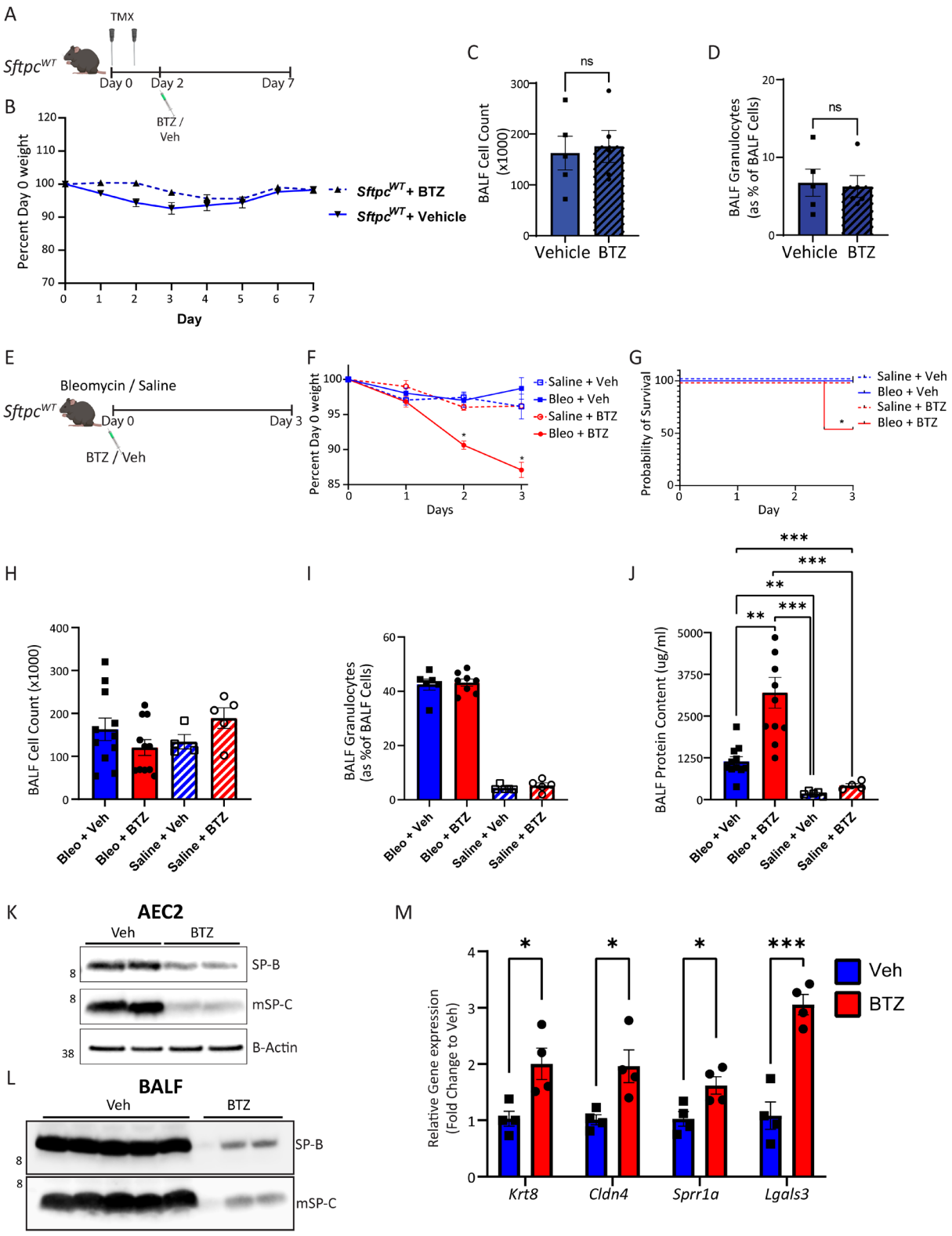

Figure S5. Proteasome inhibition accelerates mortality in Bleomycin challenged mice

(**A**) Schematic for assessment of in vivo proteasome inhibition by Bortezomib (BTZ) in *Sftpc*^{WT} mice. (**B**) Mean weight change from baseline following OG TMX given to *Sftpc*^{WT} mice followed by BTZ or Vehicle

treatment. Data are shown as mean +/- SEM (Vehicle n=5, BTZ n=8). (**C**) BALF cell counts and (**D**) percentage of BALF cells that are granulocytes determined by manually counting of Giemsa stained cytospins are unchanged in *Sftpc*^{WT} mice at 7 days after OG TMX followed by either BTZ or Vehicle treatment. (**E**) Protocol schematic for intratracheal (IT) bleomycin challenge (with Saline as vehicle control) with concurrent IP Bortezomib (BTZ) administration (with 0.1% DMSO in saline as vehicle control) in *Sftpc*^{WT} mice. (**F**) Mean weight change from baseline following IT Bleomycin/Saline to *Sftpc*^{WT} mice with concurrent BTZ or Vehicle treatment. Data are shown as mean +/- SEM (Bleomycin/BTZ n=13, Bleomycin/Vehicle n=11, Saline/BTZ n=5, Saline/Vehicle n=5) *$p < 0.05$ by mixed effect model with Tukey's multiple comparisons test. (**G**) Kaplan-Meier survival curve, *$p<0.005$ by Log-rank (Mantel-Cox) test for Bleomycin/BTZ compared to all other groups. (**H**) BALF cell counts and (**I**) percentage of BALF cells that are granulocytes by manually counting of Giemsa stained cytospins at day 3 following study initiation. (**J**) BALF protein as measured by Lowry assay showing increased BALF protein in Bleomycin treated animals with further increases with BTZ treatment. **$p < 0.005$, ***$p < 0.0005$ one-way ANOVA with Dunnett's multiple comparisons test. (**K**) Representative western blotting for SP-B and mature SP-C (mSP-C) protein in AEC2 lysate prepared from Bleomycin challenged mice treated concurrently with Vehicle or BTZ. (**L**) Western blotting of BALF large-aggregate surfactant fractions for SP-B and mSP-C showed decreased surfactant protein content in alveolar compartment of Bleomycin challenged mice with concurrent BTZ compared to Vehicle. (**M**) q-RT-PCR for AEC2 reprogramming genes *Krt8*, *Cldn4*, *Sprr1a,* and *Lgals3* from AEC2s collected at Day 3 from Bleomycin challenged mice with concurrent Vehicle of BTZ. *$p < 0.05$, ***$p < 0.0005$, by two-way t-test.

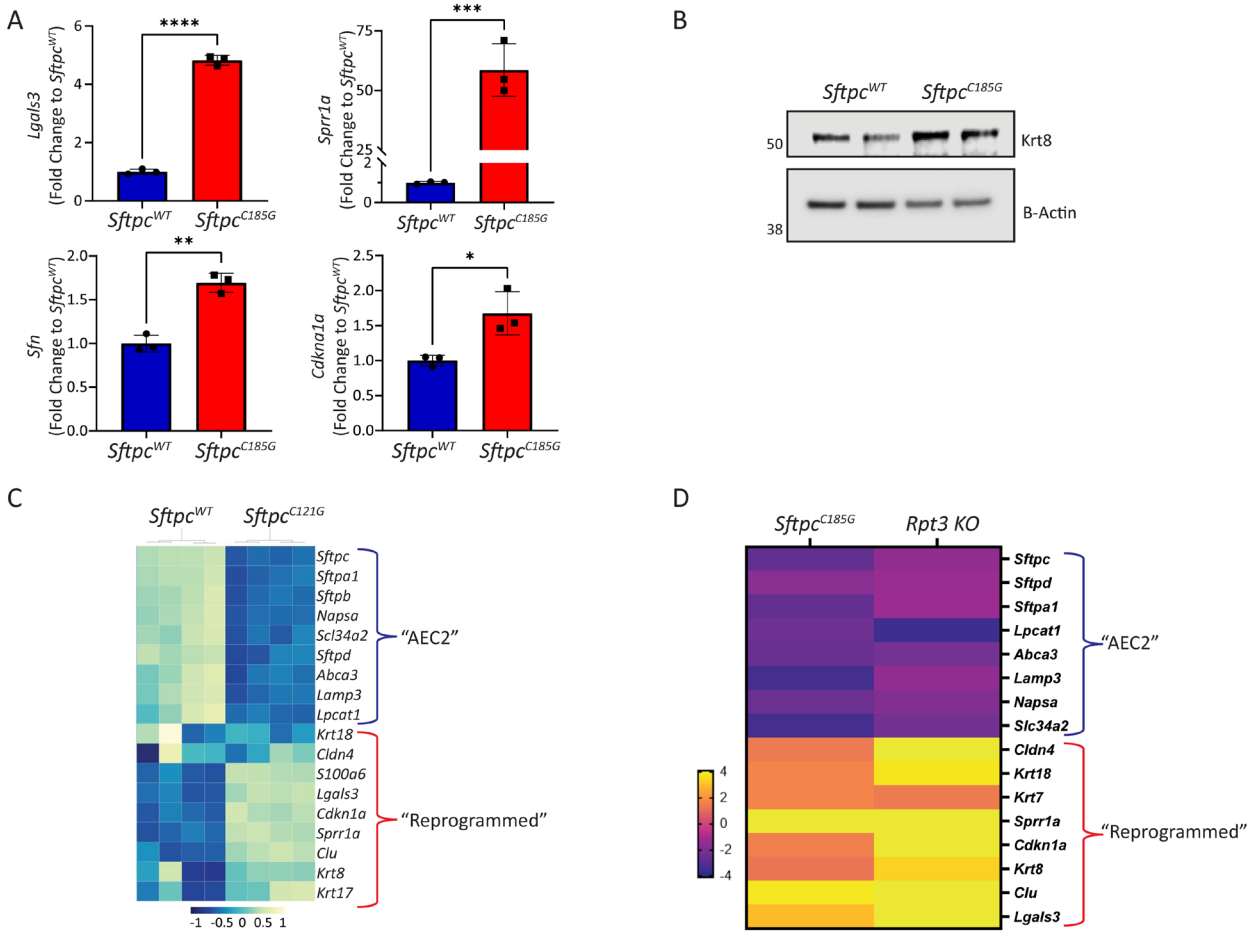

Figure S6. **Disrupted Proteostasis reprograms AEC2s**

(**A**) q-RT-PCR for AEC2 reprogramed cell state genes *Lgals3*, *Sprr1a*, *Sfn*, and *Cdkn1a* in AEC2 isolated 7 days after IP TMX administered to *Sftpc*^{WT} and *Sftpc*^{C185G} lungs. (**B**) Western blotting of AEC2 cell lysate 7 days after TMX for KRT8 shows increase in *Sftpc*^{C185G} AEC2s compared to *Sftpc*^{WT}. *p < 0.05, **p < 0.005, ****p < 0.0001 by two-way t-test. (**C**) Heatmap of selected AEC2 defining genes and markers genes for reprogrammed cell state in *Sftpc*^{C121G} model AEC2 RNA sequencing data at 5 days after TMX. (**D**) Heatmap of selected AEC2 defining genes and markers genes for reprogrammed cell state from *Sftpc*^{C185G} AEC2 and published RPT3 knockout AEC2 RNA sequencing data(11) showing fold change compared to respective control samples (*Sftpc*^{WT} for *Sftpc*^{C185G} and *Rpt3*^{Flox} for RPT3 knockout).

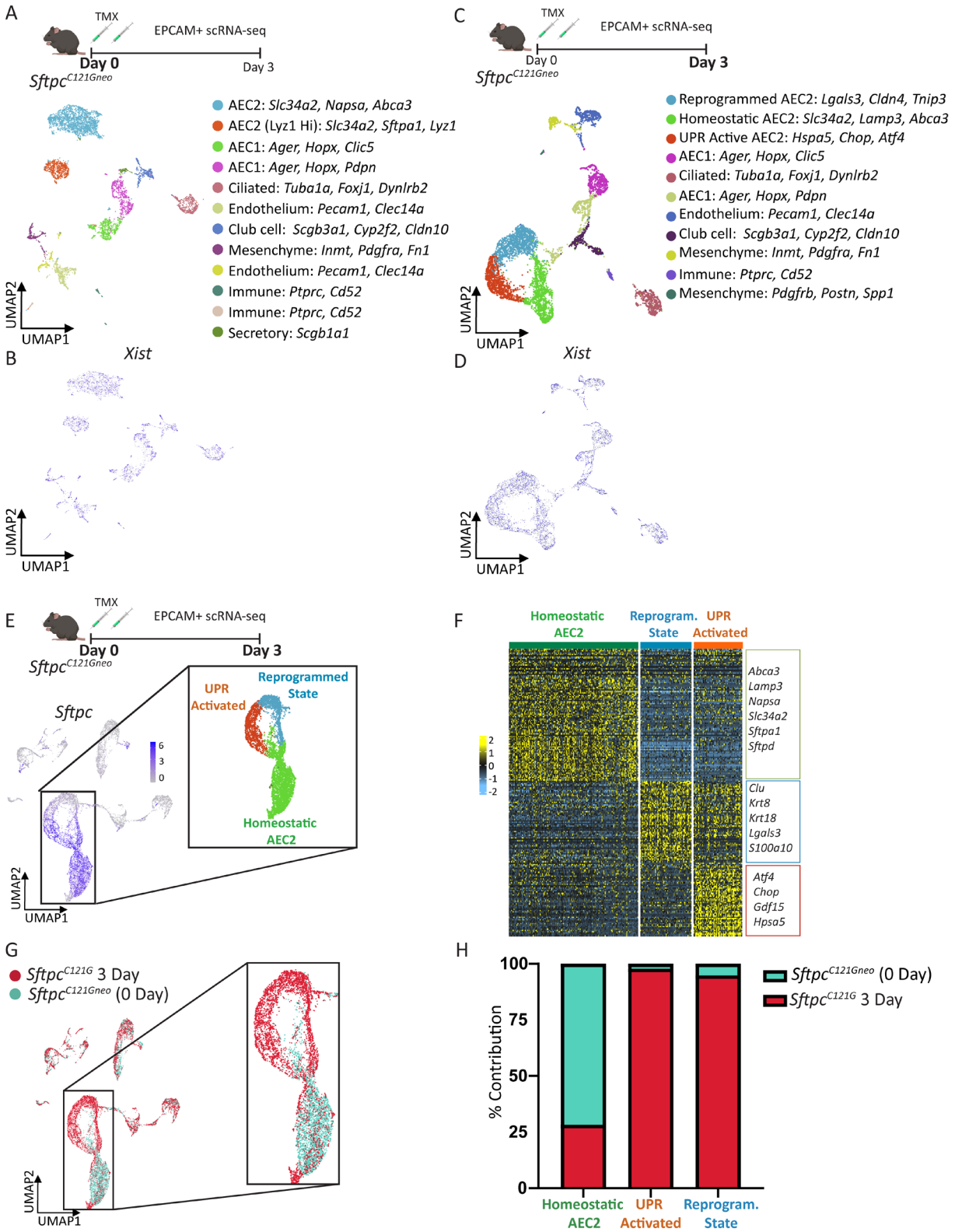

Figure S7. **Multiple AEC2 cell states emerge at 3 days post-induction of *Sftpc* mutation in mice**

(**A**) (**top**) Schematic for scRNAseq of EPCAM+ sorted cells from *Sftpc*^{C121Gneo} mice not receiving IP TMX ("0 Day") lungs and (**bottom**) UMAP projection and cluster annotation shows expected lung epithelial

populations. (**B**) Feature plots showing Xist expression reveals dispersed expression among all clusters. (**C**) (**top**) Schematic for scRNAseq of EPCAM+ sorted cells from *Sftpc*^{C121O} mice 3 Days following IP TMX ("3 Day") lungs and (**bottom**) UMAP projection and cluster annotation shows expected lung epithelial populations with 3 AEC2 clusters. (**D**) Feature plots showing Xist expression reveals dispersed expression among all clusters. (**E**) (**top**) Schematic for concatenation of 0 Day and 3 Day results and (**bottom**) UMAP projection showing 3 *Sftpc+* AEC2 state clusters. (**F**) Heatmap of the top 100 cluster defining genes by FDR for the 3 alveolar epithelial cell annotated with marker genes of each AEC2 state. (**G**) UMAP projection and (**H**) quantification of 0 Day and 3 Day epithelial contribution to the 3 AEC2 clusters.

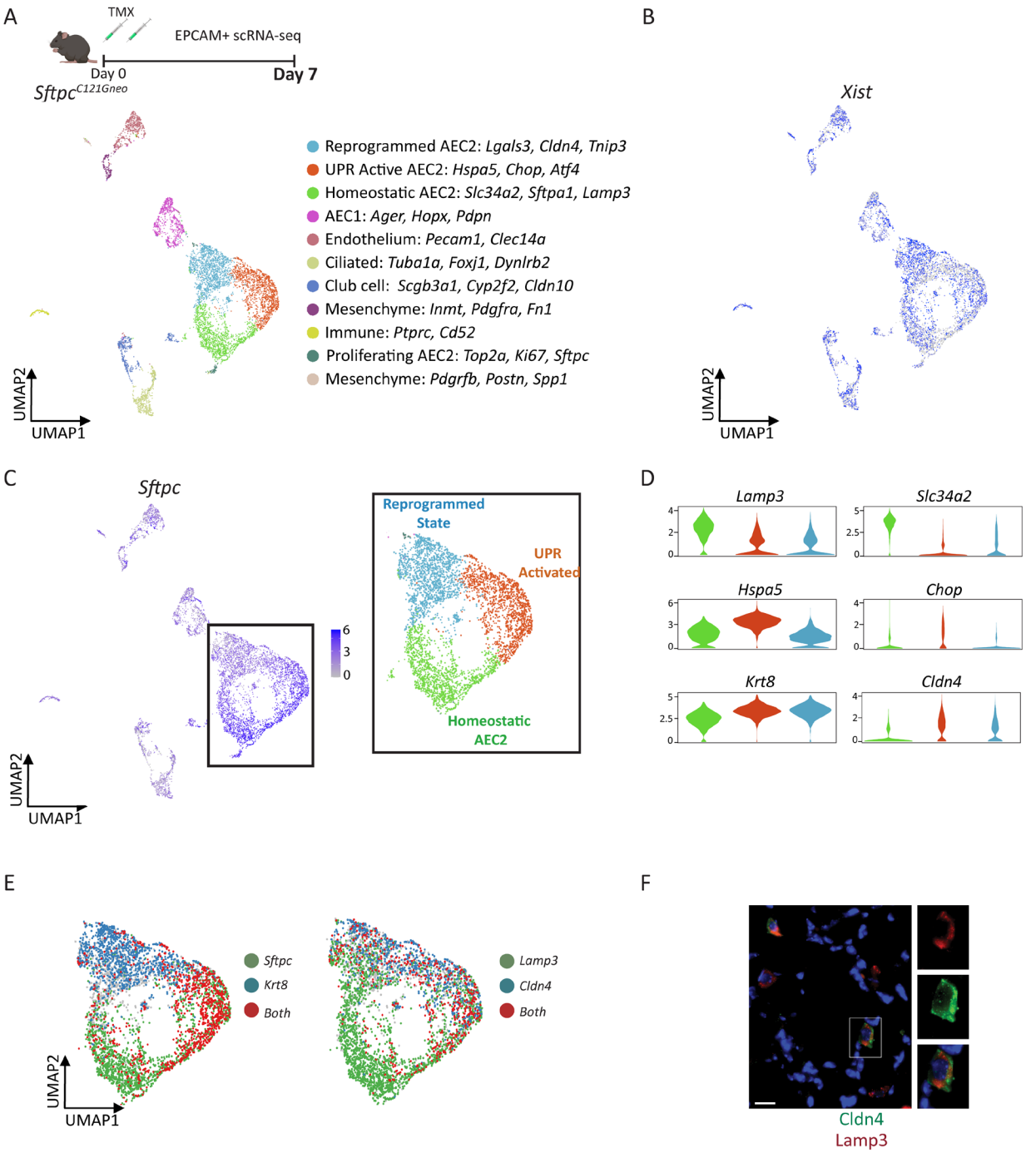

Figure S8. **Multiple AEC2 cell states persist at Day 7 post-induction of *Sftpc* mutation in mice**
(**A**) (**top**) Schematic for scRNAseq of EPCAM+ sorted cells from *Sftpc*^{C121G}mice at Day 7 following IP TMX induction and (**bottom**) UMAP projection and cluster annotation revealing expected lung epithelial populations. (**B**) Feature plots showing Xist expression reveals dispersed expression among all clusters. (**C**) UMAP projection with *Sftpc* expression in the EPCAM+ enriched *Sftpc*^{C121G} Day 7 dataset. Insert shows the 3 clusters that comprise the AEC2 states. (**D**) Violin plots of marker genes for homeostatic AEC2 state

(*Lamp3*, *Slc34a2*), UPR activation (*Hspa5*, *Chop*), and reprogrammed state (*Krt8*, *Lgals3*) in Day 3 AEC2 clusters. (**E**) (left) Biplot gene expression within the AEC2 clusters for *Sftpc* (green) and *Krt8* (blue), where cells co-expressing these genes (red) are located within the UPR activated clusters. (right) Biplot gene expression within the AEC2 clusters for *Lamp3* (green) and *Cldn4* (blue), where cells co-expressing these genes (red) are located within the UPR activated clusters. (**F**) Representative immunostaining for Lamp3 (red) and Cldn4 (green) of $Sftpc^{C121G}$ lung sections obtained 7 days post-TMX (60x magnification scale bar= 20uM).

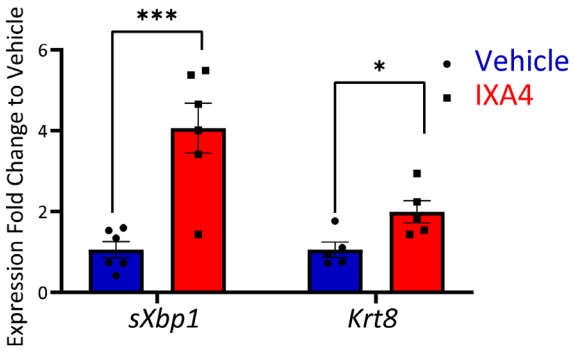

Fig S9. Stimulation of IRE1α RNase activity increases *sXbp1* and *Krt8* in MLE12 cells
q-RT-PCR of MLE12 cells treated with the IRE1 activator IXA4 at 10uM for 24 hours had increased expression of s*Xbp1* and *Krt8*. *p < 0.05 and ***p<0.0005 by two-way t-test

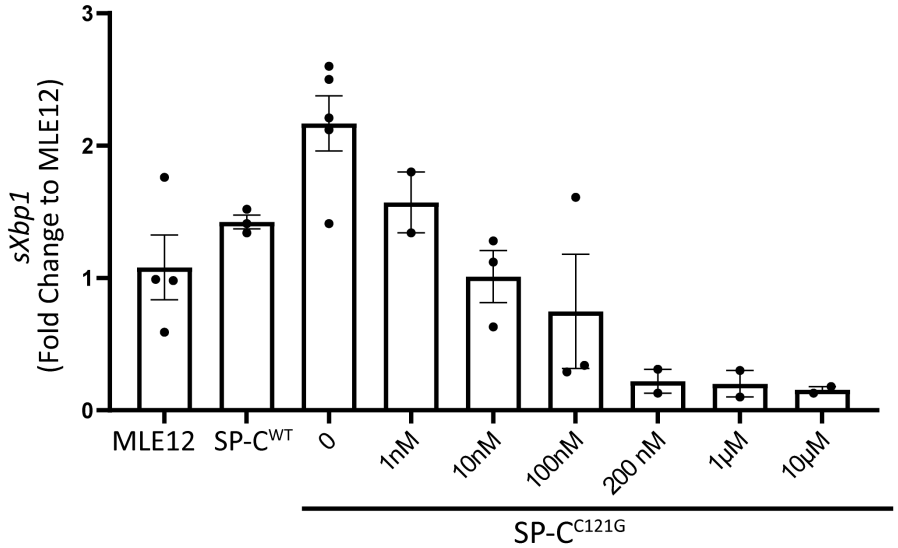

Fig S10. Dose titration of novel IRE1α inhibitor OPK-711 in MLE12 expressing mutant *SFTPC*
Dose titration of OPK-711 in MLE12 cells transfected with SP-C^{C121G} plasmid showed maximal reduction in *sXbp1* expression at 200nM.

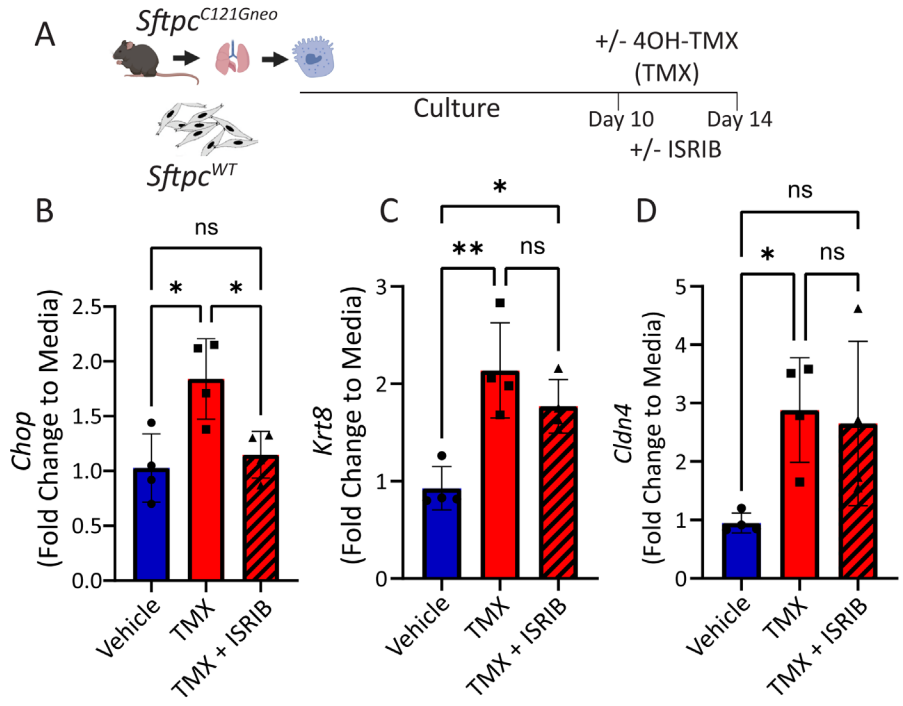

Figure S11. **Inhibition of the ISR does not reduce AEC2 reprogramming in organoid culture**
(**A**) Schematic for organoid experiments using ISRIB given concurrently with 4OH-TMX for last 96 hours of 14-day organoid culture. (**B**) *Chop* (**C**) *Krt8*, and (**D**) *Cldn4* by q-RT-PCR of day 14 organoid culture cells 96 hours comparing vehicle (0.1% EtOH + 0.1% DMSO), 4OH-TMX, and 4OH-TMX + ISRIB. N=4 biological replicates. *p < 0.05, **p < 0.005, by one-way ANOVA with Tukey's multiple comparisons test

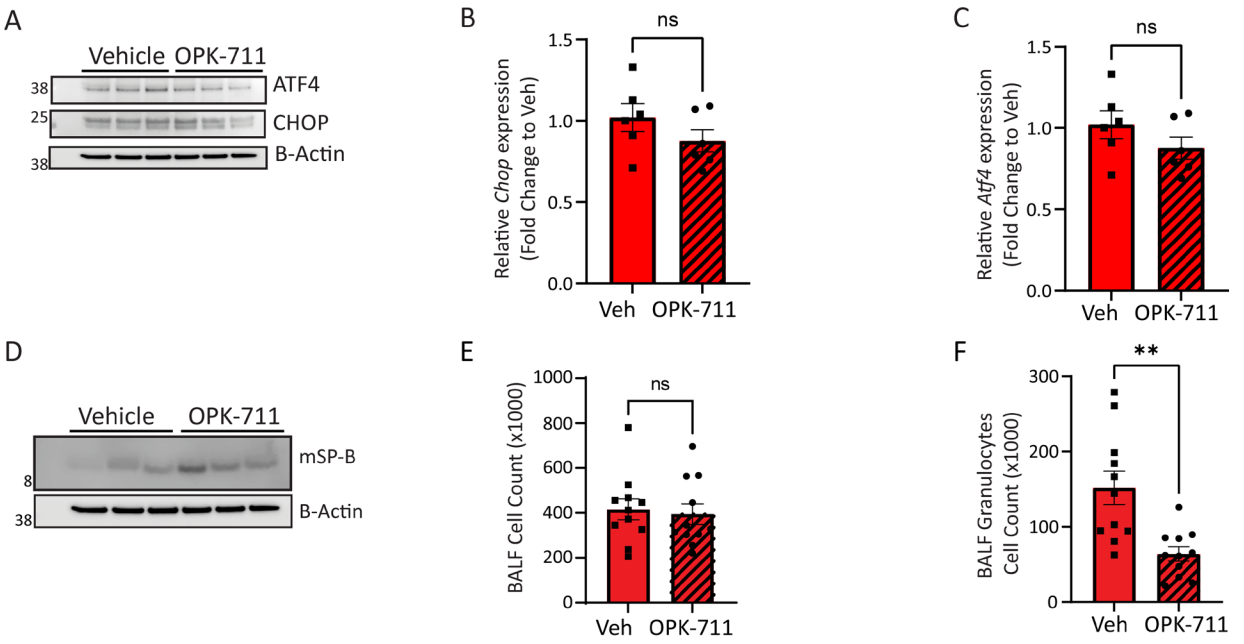

Figure S12. **IRE1α inhibition reduces AEC2 driven alveolitis, maintains surfactant homeostasis, without augmenting *Atf4*/*Chop* expression**

(**A**) Representative Western blotting of AEC2 lysates for ATF4 and CHOP from *Sftpc*^{C121G} mice treated with Vehicle or OPK-711. q-RT-PCR of AEC2 for *Atf4* (**B**) and *Chop* (**C**) from *Sftpc*^{C121G} mice treated with Vehicle or OPK-711 shows no significant effect of OPK-711 on mRNA expression. (**D**) Representative western blotting of AEC2 lysate for SP-B. Quantification of densitometry is shown in Fig 7. (**E**) Day 7 *Sftpc*^{C121G} BALF cell count is unchanged by OPK-711 compared to Vehicle, however, absolute BALF granulocytes (**F**) by manual counting of Giemsa stained cytospins is reduced with OPK-711 treatment. **p < 0.005 by two-way t-test.

Table S1. Antibodies for Western Blotting

Antibody	Clonality	Dilution	Catalog Number	Manufacturer
EGFP	Monoclonal	1:2000	632381	Living Color
ProSP-C	Polyclonal	1:3000	NPRO2	In house (12)
b-Actin	Monoclonal	1:10000	A1978	Sigma Aldrich
BiP	Monoclonal	1:1000	3177	Cell Signaling
Mature SP-C	Polyclonal	1:2500	WRAB-76694	Seven Hills Bioreagents
SP-B	Polyclonal	1:500	PT3	In house (13)
Proteosome 20s alpha	Monoclonal	1:1000	ab22674	Abcam
Proteasome 26S	Polyclonal	1:1000	140675	Abcam
ATF4	Monoclonal	1:1000	11815	Cell Signaling
CHOP	Monoclonal	1:500	5554	Cell Signaling
LC3B	Polyclonal	1:750	2775.1	Cell Signaling
Ubiquitin	Monoclonal	1:1000	04-263	Millipore
Krt8	Monoclonal	1:1000	AB_531826	DHBS Troma-I

Table S2. PCR Primers

Target	Forward	Reverse
18s	CGGCTACCACATCCAAGGAA	GCTGGAATTACCGCGGCT
Atf4	GCCGGTTTAAGTTGTGTGCT	CTGGATTCGAGGAATGTGCT
Bip	TCATCGGACGCACTTGGAA	CAACCACCTTGAATGGCAAGA
Chop	GTCCCTAGCTTGGCTGACAGA	TGGAGAGCGAGGGCTTTG
Cdkn1a	CCTGGTGATGTCCGACCTG	CCATGAGCGCATCGCAATC
Cldn4	GTCCTGGGAATCTCCTTGGC	TCTGTGCCGTGACGATGTTG
Lgals3	AGACAGCTTTTCGCTTAACGA	GGGTAGGCACTAGGAGGAGC
Krt8	TCCATCAGGGTGACTCAGAAA	CCAGCTTCAAGGGGCTCAA
Sfn	GTGTGTGCGACACCGTACT	CTCGGCTAGGTAGCGGTAG
Sprr1a	TTGTGCCCCCAAAACCAAG	GGCTCTGGTGCCTTAGGTTG
Xbp1s	AAGAACACGCTTGGGAATGG	CTGCACCTGCTGCGGAC
Xbp1u	CCTGAGCCCGGAGGAGAA	CTCGAGCAGTCTGCGCTG
Taqman Primers		
Ccl17	Mm01244826_g1	
Abca3	Mm01299912_m1	
Ccl11	Mm0041238_m1	
Cxcl1	Mm04207460_m1	
Sftpb	Mm00455678_m1	

REFERENCES

1. D. Jain *et al.*, SP-D-deficient mice are resistant to hyperoxia. *AJP - Lung Cellular and Molecular Physiology* **292**, L861-L871 (2007).
2. S. I. Nureki *et al.*, Expression of mutant Sftpc in murine alveolar epithelia drives spontaneous lung fibrosis. *The Journal of clinical investigation* **128**, 4008-4024 (2018).
3. C. W. Law, Y. Chen, W. Shi, G. K. Smyth, voom: Precision weights unlock linear model analysis tools for RNA-seq read counts. *Genome biology* **15**, R29 (2014).
4. J. Chen, E. E. Bardes, B. J. Aronow, A. G. Jegga, ToppGene Suite for gene list enrichment analysis and candidate gene prioritization. *Nucleic Acids Res* **37**, W305-311 (2009).
5. A. Dobin *et al.*, STAR: ultrafast universal RNA-seq aligner. *Bioinformatics (Oxford, England)* **29**, 15-21 (2013).
6. T. Stuart *et al.*, Comprehensive Integration of Single-Cell Data. *Cell* **177**, 1888-1902.e1821 (2019).
7. Z. Gu, R. Eils, M. Schlesner, Complex heatmaps reveal patterns and correlations in multidimensional genomic data. *Bioinformatics (Oxford, England)* **32**, 2847-2849 (2016).
8. K. Street *et al.*, Slingshot: cell lineage and pseudotime inference for single-cell transcriptomics. *BMC Genomics* **19**, 477 (2018).
9. J. A. Maguire, S. Mulugeta, M. F. Beers, Endoplasmic Reticulum Stress Induced by Surfactant Protein C BRICHOS Mutants Promotes Proinflammatory Signaling by Epithelial Cells. *Am J Respir Cell Mol Biol* **44**, 404-414 (2011).
10. D. C. Liberti *et al.*, Alveolar epithelial cell fate is maintained in a spatially restricted manner to promote lung regeneration after acute injury. *Cell Rep* **35**, 109092 (2021).
11. S. Sitaraman *et al.*, PMC6715642; Proteasome dysfunction in alveolar type 2 epithelial cells is associated with acute respiratory distress syndrome. *Sci Rep* **9**, 12509 (2019).
12. M. F. Beers, C. Lomax, Synthesis and processing of hydrophobic surfactant protein C by isolated rat type II cells. *Am.J.Physiol.(Lung Cell Mol.Physiol.)* **269**, L744-L753 (1995).
13. M. F. Beers, S. R. Bates, A. B. Fisher, Differential extraction for the rapid purification of bovine surfactant protein B. *Am.J.Physiol.(Lung Cell Mol.Physiol.)* **262**, L773-L778 (1992).